Journal of Transport Geography 78 (2019) 29–40

Contents lists available at ScienceDirect

Journal of Transport Geography

journal homepage: www.elsevier.com/locate/jtrangeo

Spatial heterogeneity in spatial interaction of human movements—Insights from large-scale mobile positioning data

Xiping Yang[a,b], Zhixiang Fang[c,*], Yang Xu[d], Ling Yin[e], Junyi Li[a,b], Shiwei Lu[f]

[a] School of Geography and Tourism, Shaanxi Normal University, Xi'an 710119, China
[b] Shaanxi Key Laboratory of Tourism Informatics, Xi'an 710119, China
[c] State Key Laboratory of Information Engineering in Surveying, Mapping and Remote Sensing,Wuhan University, Wuhan 430079, China
[d] Department of Land Surveying and Geo-Informatics, The Hong Kong Polytechnic University, Hung Hom, Kowloon, Hong Kong
[e] Shenzhen Institutes of Advanced Technology, Chinese Academy of Sciences, 1068 Xueyuan Road,Shenzhen 518005, China
[f] School of Architecture and Urban Planning, Huazhong University of Science and Technology, Wuhan 430074, China

ARTICLE INFO

Keywords:
Distance decay
Mobile phone data
Spatial interaction
Spatial heterogeneity

ABSTRACT

Distance decay is a primary characteristic of spatial interaction in human movements, and it has been incorporated into many spatial interaction models. Existing approaches mainly rely on travel survey datasets to fit the frictional coefficient of distance decay. However, limited sample size and spatiotemporal resolution make the determination of the spatial interaction characteristic from a comprehensive view difficult. Recently, this situation has been reversed due to emerging large human trajectory datasets, which have stimulated a body of literatures to re-examine the traditional issue of distance decay. However, these studies only focused on distance decay from a global perspective and neglected the spatial non-stationarity of spatial interaction. This study aims to reveal the spatial heterogeneity of distance decay of human movements extracted from massive mobile phone location data from Shenzhen, China. The power law function is utilized to fit the distance decay coefficients for inflow and outflow of each spatial analysis unit. Then, geographically weighted regression is employed to quantify the relationship between distance decay coefficients and land use distribution and between distance decay coefficients and traffic facilities. Results show that considerable spatial non-stationarity appears in the distance decay of spatial interaction, and the regression coefficients indicate the spatial variations of the influence of land use and traffic facilities on distance decay across urban space. These findings provide an in-depth insight into the distance decay characteristics of human movements in a more microcosmic space.

1. Introduction

Spatial interaction in geography is a classical concept that refers to the dynamic flows of elements (e.g., products, people, information, etc.) from one location to another (Ullman, 1980; Fotheringham and O'Kelly, 1989). The phenomenon is primarily caused by heterogeneous geographic space and the uneven distribution of elements. Elements have to be transferred among different places to balance the spatial supply and demand, and this transfer results in spatial interaction. Inspired by the gravity model, geographers have developed many variant models to determine the volume of spatial interaction between two separate places (Huff, 1963; Roy and Thill, 2004; Sen and Smith, 2012). Among these various forms, distance decay is a critical controlling factor to describe the effect of distance on spatial interaction. The role of distance can be expressed by the well-known first law of geography that states, "everything is related to everything else, but near things are more related than distant things" (Tobler, 1970). Therefore, distance decay indicates that the intensity of spatial interaction decreases with the increase in distance between places.

Human flow in cities is representative of spatial interaction because citizens must move among different places to meet the demands of everyday activities (e.g., work, shopping, and entertainment). An important task in constructing a spatial interaction model of human flow is to determine the distance decay function and distance friction coefficient. For the former, geographical researchers have developed different forms of functions to examine the law of distance decay, but power and exponential laws remain the two popular functions to model the distance decay of spatial interaction (de Vries et al., 2009; Martínez and Viegas, 2013; Halás et al., 2014; Chen, 2015). This study primarily concentrates on examining the distance decay coefficient of human spatial interaction, which plays a crucial role in improving model prediction accuracy. The decay coefficient of spatial interaction could

* Corresponding author.
E-mail address: zxfang@whu.edu.cn (Z. Fang).

https://doi.org/10.1016/j.jtrangeo.2019.05.010
Received 23 December 2018; Received in revised form 6 May 2019; Accepted 17 May 2019

be affected by the urban spatial structure (e.g., land use distribution and compactness) and flow types (e.g., commuting and shopping flows) (Fotheringham, 1981; de Vries et al., 2009; Kang et al., 2012).

A universal approach for examining the decay coefficient is to fit the distance decay function by using a sampled human flow dataset. For example, the traditional approach takes advantage of travel survey data to understand the decay characteristic of residential commuting flow, household mobility, and customer behavior in supermarkets (de Vries et al., 2009; Li and Liu, 2012; Hipp and Boessen, 2017). This individual trip dataset is often acquired through the expensive and time-consuming method of questionnaire surveys or interviews, which leads to a limited sample size. Moreover, revealing human travel behavior from a comprehensive view is difficult because of the limited temporal and spatial resolution (Yuan and Raubal, 2012; Wang et al., 2016; Siła-Nowicka and Fotheringham, 2018). However, the rapid development of information and communication technology (ICT) has brought us into the era of big data, and widespread location-aware devices can now collect a large number of human spatiotemporal trajectory datasets, such as taxi trajectories and mobile phone, social media, and smart card data (Liu et al., 2015a, 2015b). These large geo-spatial datasets encourages researchers to investigate urban human mobility at an unprecedented space–time scale, including but not limited to understanding urban spatiotemporal dynamics (Shaw et al., 2016; Sui and Shaw, 2018), detecting urban spatial structures (Liu et al., 2015a; Louail et al., 2015), exploring human commuting patterns (Ma et al., 2017; Yang et al., 2018a), and quantifying human activity space (Xu et al., 2016).

Recently, studies have been conducted on the traditional issue of distance decay in human movements by utilizing emerging human sensing datasets. The main contents can be traced from two threads. The first thread reviews the decay law of human mobility and constructs corresponding prediction models (González et al., 2008; Song et al., 2010; Liu et al., 2012). The second thread re-examines the decay coefficient of human spatial interaction and calibrates the typical spatial interaction model by using new trajectory datasets (Kang et al., 2012; Yue et al., 2012; Gao et al., 2013; Wang et al., 2016; Han et al., 2018; Siła-Nowicka and Fotheringham, 2018). Most of these extant studies provided an understanding of the distance decay of spatial interaction only from a global perspective, and the decay coefficient was regarded as homogeneous for an entire city. Only a few studies have considered spatial non-stationarity when fitting the distance decay parameters (Fotheringham Stewart et al., 1996; Suárez-Vega et al., 2015), but both of the two studies used the limited survey datasets and either focused on visual analysis or locating a new store using Huff model, which is different from our consideration. In addition, Kordi and Fotheringham (2016) proposed a spatially weighted interaction models for detecting, visualizing and analyzing spatial non-stationarity in spatial interaction processes, but they primarily focused on modelling the flows between two places using spatially weighted techniques rather than examining the spatial variations of distance decay coefficients. Kong et al. (2017) utilized taxi data to investigate the public facility characteristic from a spatial interaction perspective, but they only analyzed the distance decay of visiting urban hospitals and limited in examining the influence factors of distance decay. This study intends to enrich existing literature by investigating the spatial variations of distance decay in spatial interaction and quantifying the spatial varying influence of land use characteristics and traffic facilities on the intensity of distance decay. The heterogeneous geographic space makes it impossible for the whole space to have the same decay velocity in spatial interaction, especially in an urban space with an uneven distribution of population, land use, and infrastructure. This absence of literature may be attributed to the low coverage rate and spatial resolution of traditional individual survey data. At present, large human-tracking datasets provide a new opportunity for acquiring an in-depth understanding of human spatial interaction at a highly detailed spatial scale.

This study aims to address this gap by revealing the spatial variations of distance decay in urban space through the use of massive mobile phone location data from Shenzhen, China. First, the human movement trips is extracted from the individual space–time trajectory constructed from mobile phone location records. Second, we distinguish the incoming and outgoing flows of a location and fit the distance decay coefficients by using a power law function for its inflow and outflow, respectively. The decay parameters are discussed from statistical and spatial perspectives. Finally, ordinary least-squares (OLS) regression and geographically weighted regression (GWR) are performed to explore the relationship among distance decay coefficients, land use distribution, and traffic facilities. The results indicate that considerable spatial variations exists in the influence of land use and traffic factors on the intensity distance decay. These findings provide us an improved understanding of the distance decay of human movements at a micro-cosmic scale.

The remainder of this paper is arranged as follows. Section 2 introduces the study area and mobile phone data used in this work. Section 3 provides a description of the study's methodology ranging from the extraction of the origin–destination trips matrix and estimation of distance decay coefficients to the description of the GWR model. Section 4 shows the regression results of OLS and GWR and discusses the spatial varying relationship between distance decay and the explanatory variables related to land use and traffic. The last section presents the conclusions of this study and discusses further work directions.

2. Study area and dataset

2.1. Study area

The case study area, namely, Shenzhen, is located in the southeast of China and adjacent to Hong Kong. Shenzhen is the first special economic zone established after the implementation of the reform and opening-up policy in China. With the rapid development in the past 40 years, Shenzhen has become a national economic, financial, technological, and innovative center and one of the largest cities in China. Shenzhen covers a total area of approximately 2000 km^2 with a population of approximately 20 million. Fig. 1 shows Shenzhen, which contains 10 administrative districts. Futian, Luohu, and Nanshan are well-developed areas (i.e., downtown areas) dominated by numerous commercial, financial, and high-tech enterprises. Banan, Longhua, and Longgang are suburbs and dominated by many industrial parks and factories. Yantian is an international port for marine trade. The other three districts (Guangming, Pingshan, and Dapeng) are rural areas and contain several villages and tourist destinations. Note that the islands in the left bottom are not considered in the following analysis.

2.2. Dataset

Regular sampling mobile phone location data were used in this study to capture human movement trajectories. Unlike detailed call record (CDR) data that sample individual locations only when communication activities (e.g., phone call or text messages) occur, this dataset captures individual locations at regular intervals (approximately 1 h) and covers a total of digital footprints of approximately 16 million mobile phone users on a typical workday in 2012. Each record contains four essential attributes, namely, user ID, recording time, and longitude and latitude of the corresponding cell phone tower that provides service to the mobile phone. Table 1 shows an example of individual records during a workday, and the time window represents the record occurring time slots. Notably, the dataset has been encrypted for privacy protection before allowing it to be used for research. More than 5900 distinct cell phone towers were extracted from the dataset, and voronoi polygons were produced based on the locations of cell phone towers to denote the service area of towers (Yang et al., 2018a).

The four other spatial datasets used in this study were urban land

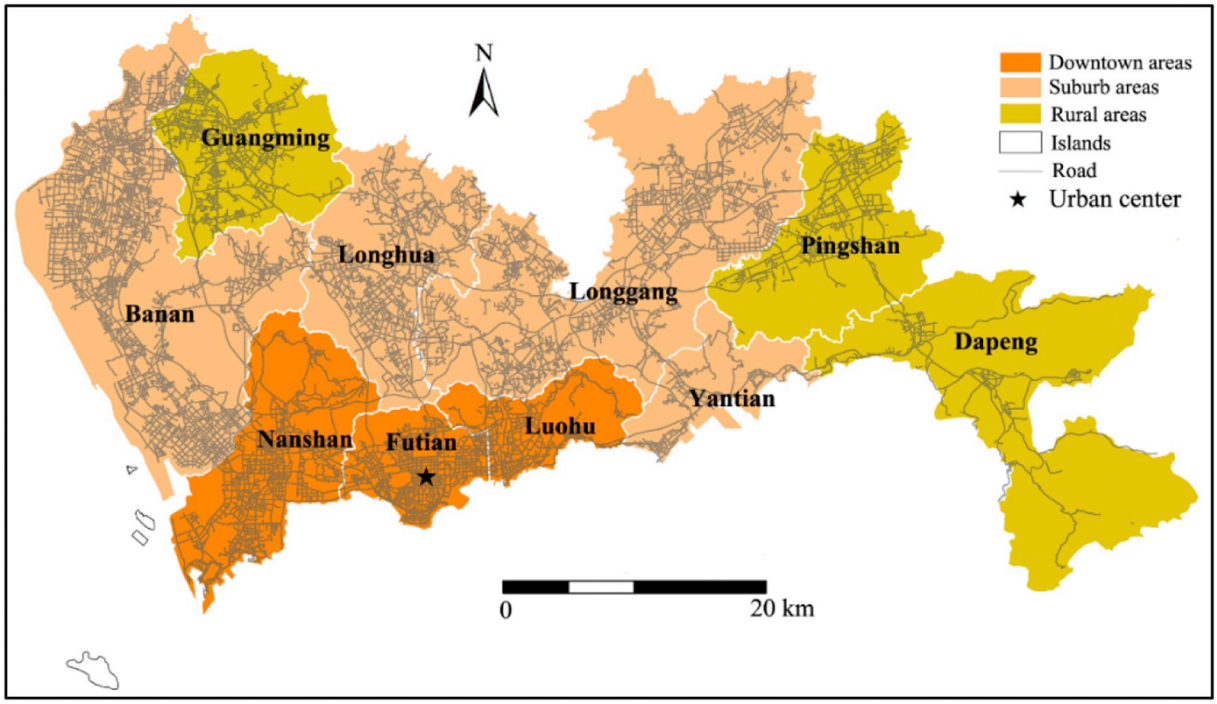

Fig. 1. Study area.

Table 1
An individual's cell phone records in a day.

User ID	Record time	Time window	Longitude	Latitude
3y8k6g6******	00:35:38	00:00–01:00	113.***	22.***
3y8k6g6******	01:30:45	01:00–02:00	113.***	22.***
3y8k6g6******	02:23:20	02:00–03:00	113.***	22.***
3y8k6g6******	…		…	…
3y8k6g6******	23:41:58	23:00–24:00	113.***	22.***

use, road network, bus stations, and subway. Land use data included 53 land use types, which were aggregated into six categories based on the planning standards of urban development land. The six categories were commercial (wholesale, retail, financial land, etc.), industrial (industrial parks, factories, warehouses, etc.), residential, public (hospitals, education, open green parks, etc.), transport (airport, railway stations, ports, etc.), and other lands (agricultural, military, special, etc.). The six kinds of land use were employed to quantify the effect of land use distribution on the distance decay of human movements. Road networks, bus stations, and subways were used to measure the effect of public traffic facilities on distance decay.

3. Method

First, we extracted the human movement trips matrix from the mobile phone data. Second, the process for estimating the coefficients of distance decay was introduced for each traffic analysis zone (TAZ). Finally, we described the GWR model and explanatory variables to be inputted into this model.

3.1. Extracting human movement trips from mobile phone dataset

For each mobile phone user, we can establish a 3D space–time trajectory by linking all location records in a chronological order (Fig. 2). According to the theory of time–geography (Hägerstraand, 1970), the horizontal plane represents the spatial longitude and latitude of cell phone towers, and the vertical plane represents the updated time of records. The space–time trajectory can be expressed as follows:

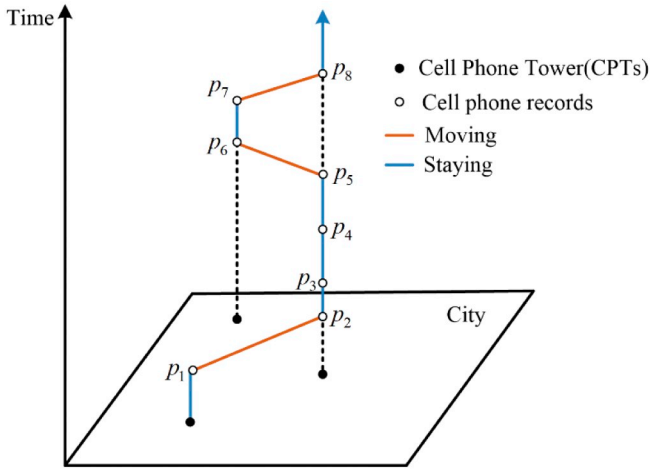

Fig. 2. Space-time trajectory of a mobile phone user.

$$T = [p_1, p_2, \cdots, p_i, \cdots, p_n], \quad p_i = (x_i, y_i, t_i, id_i) \tag{1}$$

where p_i represents the ith record point; x_i, y_i, and t_i represent the longitude, latitude, and time of the point, respectively; and id_i denotes the ID of the cell phone tower. In order to extract human movement trips, it is necessary to identify the stop locations from the space-time trajectory. We scanned the space–time trajectory points successively from the first point to the end point. When the tower ID of the two adjacent tracking points are identical ($id_i = id_{i+1}$) and the duration time is greater than 0.5 h (regular sampling interval of the dataset is approximately 1 h), a stop can be identified at cell phone tower id_i (blue line in Fig. 2), then the movement between two adjacent stops can be considered as a trip and the two stops are labelled as the origin and destination of the trip respectively based on their temporal order (orange line in Fig. 2). In this manner, we can extract all movement trips for all cell phone users and generate an cell phone tower-based origin-destination flow matrix, which is denoted as $(id_i, id_j, count_{ij})$, where $count_{ij}$ represents the number of trips flowing from the tower id_i to id_j during the day.

In this study, the traffic analysis zones (TAZs) were utilized to implement the analysis of distance decay. As a basic spatial analysis unit, TAZ has been widely used by geographers to conduct traffic surveys, trips generation forecasting, human mobility patterns and community planning (Fang et al., 2017). Therefore, the extracted tower-based flows should be aggregated into TAZ-based movement flows. This study allocated the tower-based flows according to the proportion of overlapping areas between voronoi polygons and TAZs. Referring to the study by Yin et al. (2015), the formula can be described as follow:

$$OD_{ij}^{TAZ} = \sum_{m=1}^{N}\sum_{n=1}^{N}\frac{A_i^m}{A^m}\cdot\frac{A_j^n}{A^n}\cdot OD_{mn}^{tower} \quad (2)$$

where A_i^m represents the overlapping area between voronoi polygon m and TAZ i, A_j^n represents the overlapping area between voronoi polygon n and TAZ j. A_m and A_n represent the area of voronoi polygon m and n respectively, OD_{mn}^{tower} represents the tower-based flows from voronoi polygon m to voronoi polygon n. N is the number of cell phone towers. For each TAZ, human flows can be separated into inflow and outflow. Inflow represents the number of people moving from other TAZs to this TAZ, and outflow represents the number of people leaving the TAZ to other TAZs. This study would investigate the distance decay of inflow and outflow for each TAZ respectively.

3.2. Estimating the coefficients of distance decay of human movement trips

The number of flowing people decreases with the increase in distance between two places. Previous studies have tried to model the distance decay of human movements using human travel data, and the main debate that remains is between power and exponential laws (de Vries et al., 2009; Chen, 2015). In fact, the effectiveness of models depends on the dataset used in the research. Kang et al. (2013) compared the human movements of Singapore by using mobile phone and taxicab data and found that mobile phone movements are inclined to follow a power-law function, whereas taxicab trips follow an exponential distribution (Kang et al., 2013). Therefore, this study employed the power-law function to model the distance decay of human movement trips for each TAZ. The power-law function can be represented as

$$P(d) = d^{-\beta} \quad (3)$$

$$ln(P) = -\beta\cdot ln(d) \quad (4)$$

where P represents the cumulative distribution of trips moving at distance d between two places. β is the coefficient of distance decay that indicates the influence of distance on human interaction between two places; a large value indicates that distance has a considerable effect on human flows (Gao et al., 2013; Liu et al., 2014). To calculate parameter β, a logarithm function was applied to both sides of Eq. (3) to transform it into a linear mode. The slope of the line reflects how fast the distance decays. The OLS method was used to fit the regression coefficient of the linear model. The distance decay coefficients of inflow and outflow, which are denoted as $inflow\_\beta_i^{TAZ}$ and $outflow\_\beta_i^{TAZ}$ respectively, were fitted for TAZ i by using the above model. The distance decay coefficients of TAZs were adopted as dependent variables in the following GWR analysis.

3.3. Geographically weighted regression analysis

To investigate spatial heterogeneity of the distance decay of spatial interaction, this study employed the GWR model to quantify the relationship among the coefficients of distance decay, local land use characteristics, and traffic facilities. This section presents a brief description of the GWR model and the corresponding explanatory variables.

Given that a spatial surface is homogeneous, the traditional global multivariate regression model is often used to explore the relationship between dependent and independent variables. The formula of this regression model is

$$Y_i = \alpha_0 + \sum_k \alpha_k X_{ki} + \varepsilon_i \quad (5)$$

where Y_i represents the dependent variable, α_k is the estimated coefficient of the independent variable X_{ki}, and ε_i is the residual. The OLS method is generally applied to estimate the coefficients. The estimated regression coefficients are identical and constant for the entire study area due to the globalism of this model. However, the entire area cannot be completely homogeneous because heterogeneity widely exists in spatial data and highly depends on the spatial characteristics of local regions. The GWR model can quantify the spatial effect by embedding geographical coordinates into the global OLS regression model. The general GWR model is given as follows:

$$Y_i = \alpha_0(u_i, v_i) + \sum_k \alpha_k(u_i, v_i)X_{ki} + \varepsilon_i \quad (6)$$

where (u_i, v_i) represents the coordinate of location i and $\alpha_k(u_i, v_i)$ is the regression coefficient of independent variable X_{ki} at location i. Weighted least squares is used to estimate the coefficients of the GWR model, where the weights capture the spatial effect of local observations on the observation at location i. The popular Gaussian kernel function is employed to calculate the spatial weighted matrix; it models the spatial effects of surrounding observations by Gaussian distance decay within the bandwidth. Notably, bandwidth selection is critical because it has a great impact on the estimation of coefficients. A corrected Akaike information criterion (AICc) is used to evaluate the fitting to select the optimum bandwidth (Burnham and Anderson, 2004). Owing to the incorporation of the spatial weighted matrix for estimating regression coefficients, the GWR model can generate varying regression coefficients across the study area according to local spatial characteristics. Therefore, we utilized this method to measure the spatial variations in the relationships among distance decay of human movements, land use distribution, and traffic convenience.

The explanatory variables were mainly derived from land use and transport, which are strongly associated with human mobility. We calculated the percentage of the six types of land use (commercial, industrial, residential, public, transport, and others) for each TAZ to indicate the land use distribution characteristics within the TAZ. The mixture of land use types is an important impact factor on human travel. Entropy was employed to assess the mixture of land use in each TAZ, and the specific formula has been provided in a previous study (Tu et al., 2018; Yang et al., 2018b). With regard to transport convenience, we utilized road density, bus stop density, and distance from TAZ to the nearest subway station to evaluate the degree of traffic convenience for each TAZ. Road density is defined as the length of road links within TAZ divided by the area of the TAZ. Bus stop density is defined as the number of bus stops within TAZ divided by the area of the TAZ. The distance from the center of TAZ to the nearest subway station was calculated by using Euclidean distance. In addition, the location of TAZ in the city was regarded as an explanatory variable, which is measured by the Euclidean distance between the center of TAZ and the urban center. Moreover, we counted the number of service mobile phone users for each tower during the day, and aggregated the these users into TAZs according to the proportion of overlapping area between voronoi polygons and TAZs, which could be considered as a population-related explanatory variable, denoted as population. In total, 12 explanatory variables were considered initially.

For a comparative analysis, traditional OLS and GWR models were applied to inflow and outflow, respectively. Therefore, four regression models were implemented to explore the relationship between distance decay of human movements and the proposed explanatory variables related to land use and transport. The four models are denoted as inflow_OLS, inflow_GWR, outflow_OLS, and outflow_GWR. The software developed by Nakaya et al. (2009) was used to implement the

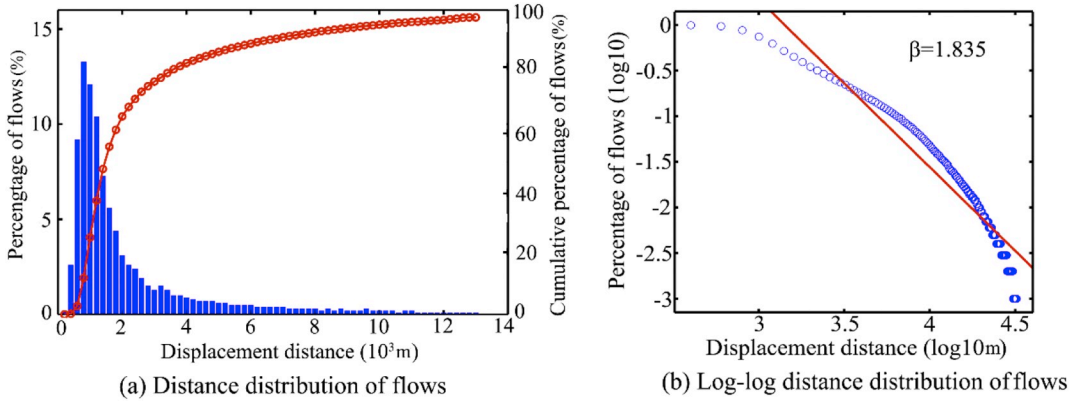

Fig. 3. Displacement distance distribution of flows.

GWR analysis, and all explanatory variables were normalized by using the z-score to eliminate the influence of magnitude.

4. Results and discussion

4.1. Distance decay characteristic of human movements

4.1.1. Global distance decay characteristic

On the basis of the extracted TAZ-based flows matrix, we first checked the global distance decay distribution of Shenzhen. Fig. 3a shows the frequency and cumulative distance distribution of movement flows (binwidth = 0.5 km). More than 80% of the displacement distance between the origin and destination was less than 4 km. The frequency distribution followed a long-tail law, which demonstrates that only few displacements move across a long distance. Fig. 3b shows the log-log distance distribution of movement flows. A liner model was utilized to fit this distribution (red line in the Figure), the goodness of fit R-square was 0.902 and the generated global distance decay parameter β was 1.853, which is larger than the findings of Harbin (1.60) but less than the value for Singapore (2.5) (Gao et al., 2013; Kang et al., 2013). The difference may be attributed to the discrepancy in spatial analysis units (voronoi polygons for Harbin, regular grid cells for Singapore) and urban spatial structure characteristics (e.g., urban morphology, functional zone distribution, compactness, etc.).

4.1.2. Local distance decay characteristics

Before fitting the decay coefficients, we calculated, for each TAZ, the number of TAZs that interact with it (e.g., ones that have inflow/outflow interaction with that selected TAZ). Fig. 4 displays the statistical distribution of number of interacting TAZs from both the perspective of inflow and outflow. This gives us an idea about the sparsity of interactions for all the TAZs, from both the perspective of inflow and outflow. For TAZs with little interactions with others, it would be problematics in fitting the distance decay function. To mitigate this issue, we choose to filter TAZs with number of interacting TAZs less than 20 for inflow, and the same for outflow.

For each TAZ, the inflow and outflow of distribution in displacement decay were fitted to generate decay coefficients $inflow\_\beta_i^{TAZ}$ and $outflow\_\beta_i^{TAZ}$ of the TAZ, respectively. Fig. 4 presents the statistical distribution of decay coefficients and the goodness of fit. For goodness of fit (Fig. 5b and d), more than 85% of the TAZs had values greater than 0.8 regardless of inflow or outflow, which indicates that the power law can capture the distance decay distribution to some extent. The decay coefficients shown in Fig. 5a and c show a similar Gaussian normal distribution, and the peak corresponds to decay coefficient $\beta = 2.0$. The percentages of coefficients between 1.5 and 2.5 were 80.3% and 84.3% for inflow and outflow, respectively, and the distribution of the decay coefficient of inflow was slightly more decentralized than that of outflow (Fig. 5a and c). Therefore, it can be concluded that the intensity of distance decay is not consistent for the entire city but varies for different places.

From the perspective of spatial distribution, human movements in the TAZs located in the northern part of Shenzhen decayed faster than that in the southern part, especially in the northwest part (Fig. 6). As aforementioned, the three suburbs of Baoan, Longhua, and Longgang are characterized by a large number industrial parks and factories, and many workers are likely to live in places near their workplaces or in dormitories provided by factories to save commuting time and cost (Xu et al., 2015). As a result, people living in the northern parts tend to have a smaller activity space than those living in the southern parts, which may be an explanation for the faster distance decay in the northern parts. In addition, it can be seen that the spatial distribution of decay coefficients based on inflows and outflows are unsymmetrical. We conjecture that one major reason for this may be caused by human trips chain of the day. For example, it is possible that one takes a trip from home to workplace in the morning, he may travel to another place to take activities such as dinner or recreation after finishing one day's work, then he returns to home from this place. In this case, he doesn't

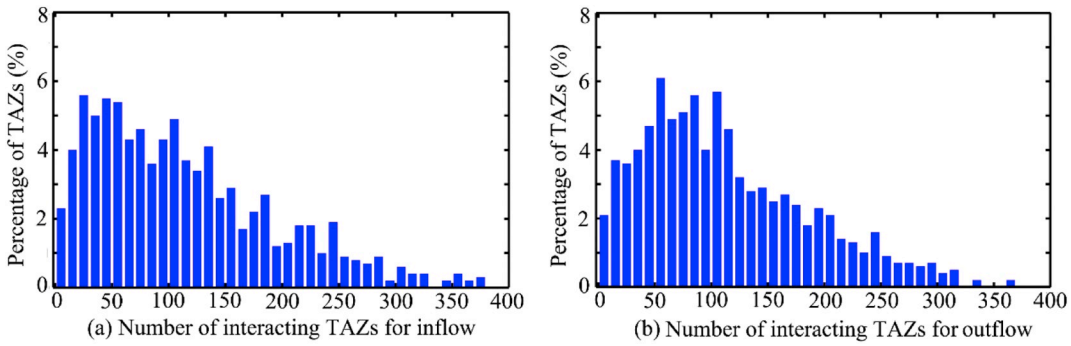

Fig. 4. The statistical distribution of number of interacting TAZs from both the perspective of inflow and outflow. (binwidth = 10).

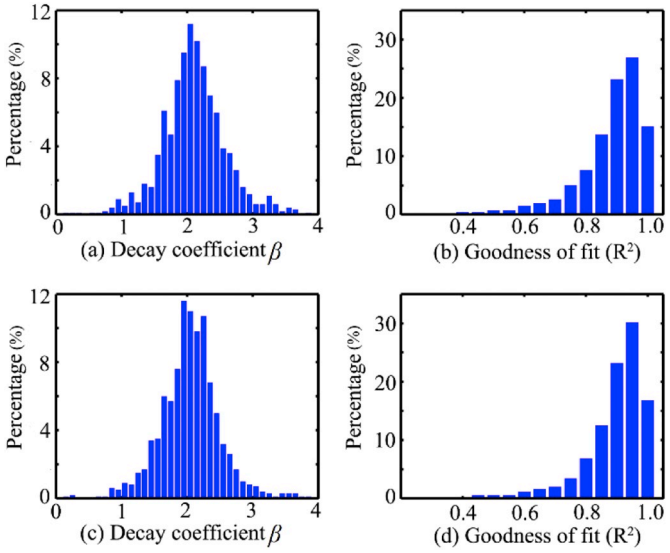

Fig. 5. Distribution of decay coefficients (β) and goodness of fit (R^2) values.

directly return to home from workplace, which may lead to the unsymmetrical spatial distribution of decay coefficients for inflow and outflow. We utilized the global Moran's I index to test the spatial autocorrelation of distance decay coefficients (Table 2). The results showed that remarkable spatial clustered patterns existed in inflow and outflow. Therefore, the GWR model is more appropriate than the global OLS model for regression analysis.

4.2. Impact factors of distance decay

4.2.1. Regression analysis of the OLS model

We employed the global OLS model to examine the effect of land use and traffic facilities on the distance decay of spatial interaction. It is infeasible to use all of these six categories of land use for regression analysis because the sum of these land use is one, thus we excluded the last category (i.e., other lands) of land use type to avoid multicollinearity, and this category includes some land use (agricultural, military, special lands), which might be less related with human activities. After that, we executed a multicollinearity test (Tu et al., 2018; Qian and Ukkusuri, 2015), and the other 11 independent variables remained for the subsequent regression analysis. Table 3 displays the regression results of Inflow_OLS and Outflow_OLS models. According to the adjusted R^2, these selected land use- and traffic-related independent variables only explained 4.6% and 5.9% of the variation in the distance decay parameter of inflow and outflow, respectively.

At a global level, the land use-related independent variables had a remarkable impact on distance decay, whereas only subway (D_1) of the three traffic-related variables had a significant association with distance decay of inflow. Regardless of inflow and outflow, an increase in the percentage of the industrial or residential land of a TAZ would improve the intensity of distance decay in spatial interaction, while an increase in transport land would decrease the intensity of distance decay. The incremental transport land may enhance the residential travel distance and make the distance decay slow. A TAZs with larger population may be more active, which is likely to attract or disperse people at a large scale, thus the distance decay of spatial interaction may be slower. A main difference between inflow and outflow was observed in commercial, public land and D_2, which generated a remarkable positive impact on the distance decay coefficient of outflow but not on that of inflow, indicating that the three variables would make people tend to take their activities in local area. Moreover, when the location of a TAZ was closer to the nearest subway station, distance decay of inflow was slower, which indicates that the subway stations would improve the range of attraction of the TAZ. However, we do not anticipate that a place with high mixed land use would provide many chances for people doing different activities (e.g., work, shopping, recreation, etc.), and they do not need to travel long distances to meet their life demands. Therefore, the distance decay of outflow should be faster than that with less land use mix. A possible explanation for this counterintuitive phenomenon is that TAZs with high land use mix are concentrated around the urban center, which may generate a global attraction or radiation for the entire city.

Although the OLS regression was able to provide a global understanding of the relationship between distance decay and land use characteristics and traffic facilities, some counterintuitive conclusions still prevail. For example, the results indicated that traffic facilities were little related with distance decay, and the explanation capability of the model was very weak. This result may have been caused by overlooking the spatial non-stationary of these explanatory variables. The Koenker (BP) statistic was used to determine if a consistent relationship exists between independent and dependent variables in geographic and data spaces. The statistically significant result indicated that each explanatory variable exhibited significant non-stationarity, demonstrating that the GWR model was more suitable for regression analysis than the OLS model (Lee and Schuett, 2014; Liang et al., 2018). After employing the toolbox of Arcgis 10.2, the BP statistics of inflow and outflow were determined to be 55.493 and 44.175, respectively, with an identical p-value of 0.000. Therefore, we further explored their relationship via GWR analysis.

4.2.2. Results of GWR model

The estimated results of Inflow_GWR and Outflow_GWR are shown in Tables 4 and 5, respectively, which list the descriptive statistics of the varying regression coefficients, namely, minimum, lower quartile,

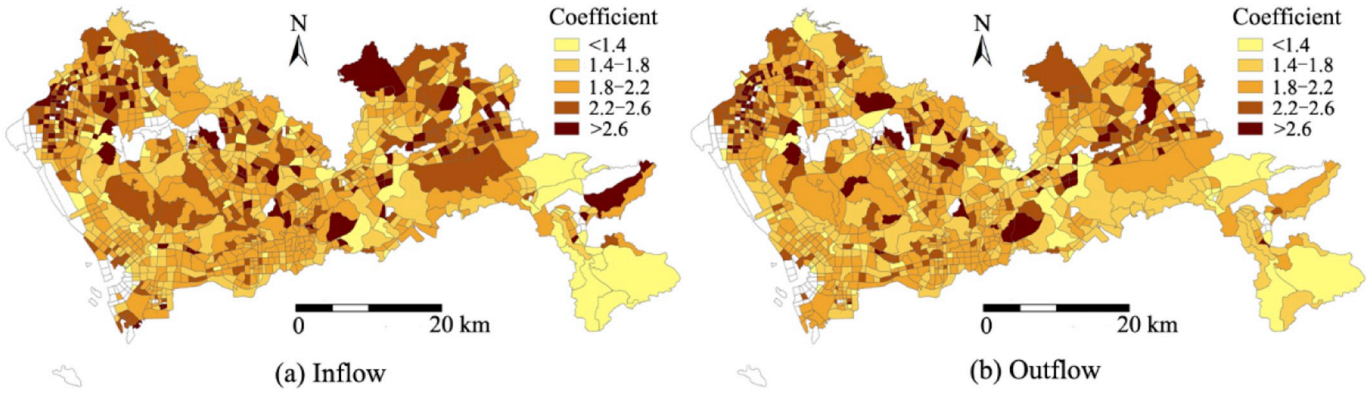

Fig. 6. Spatial distribution of decay coefficients for TAZs.

Table 2
Global Moran's I test for spatial autocorrelation analysis of distance decay coefficients.

	Moran's I index	z-Score	*p*-Value
Inflow	0.349	7.943	0.000
Outflow	0.355	7.919	0.000

Table 3
Regression result of the global OLS model.

Dependent variable	Model			
	Inflow_OLS		Outflow_OLS	
Independent variable	Coefficient	t-Statistic	Coefficient	t-Statistic
Commercial	0.002	0.092	0.039	2.167[b]
Industrial	0.094	4.029[c]	0.114	5.300[c]
Residential	0.070	2.566[c]	0.096	3.788[c]
Public	−0.002	−0.087	0.033	1.893[a]
Transport	−0.042	−2.031[b]	−0.032	−1.691[a]
Mixed land use	−0.006	−0.229	−0.042	−1.745[a]
Road density	0.006	0.211	0.009	0.379
Bus stop density	−0.000	−0.017	0.003	0.165
Distance to the nearest subway station (D_1)	−0.056	−2.161[b]	−0.024	−1.011
Distance to the urban center (D_2)	0.043	1.562	0.044	1.721[a]
Population	−0.060	−3.359[c]	−0.054	−3.272[c]
R^2	0.056		0.069	
Adjusted R^2	0.046		0.059	

[a] Represents the significance of the regression coefficient at the 0.1 level.
[b] Represents the significance of the regression coefficient at the 0.05 level.
[c] Represents the significance of the regression coefficient at the 0.01 level.

median, upper quartile, maximum, and standard deviation (Std). In comparison with the global OLS model, the remarkably improved adjusted R^2 from 4.6% and 5.9% of the OLS model to 20.6% and 23.1% of the GWR model for inflow and outflow respectively, which illustrates that the GWR model performed better in fitting the distance decay coefficient and selected explanatory variables. The descriptive statistical indexes provide a general understanding of the distribution characteristics of regression coefficients (Tables 4 and 5). For example, large standard deviation values indicate that the distribution of coefficients of D_1 and D_2 is more dispersed than that of the other variables. For industrial and residential, more than 75% of TAZs had a positive effect on distance decay, whereas transport and land use mix in most TAZs had a negative effect on distance decay. Next, we investigated the spatial variations effect of these explanatory variables on distance decay by projecting these coefficients on the TAZs.

Fig. 7 shows the spatial distribution of estimated coefficients of GWR for inflow and outflow. The red color indicates that the corresponding explanatory variables have a positive influence on distance decay, and the blue color represents a negative influence. The deeper the color is, the greater the influence is. The GWR model could quantify the spatial varying influence of each independent variable on distance decay. The intensity of distance decay of human inflow and outflow for each TAZ could reflect the potential range of attraction and radiation of the place. A small decay coefficient may indicate that the place could attract or radiate people from or to farther places. Even for the same independent variable, the spatial distribution of influence presented a difference between inflow and outflow (Fig. 7). We analyzed the spatial characteristic of the influence of each explanatory variable for inflow and outflow.

For land use-related variables, the influence of commercial land exhibited some differences in spatial distribution between inflow and outflow. The positive values for inflow were mainly distributed in Baoan, Nanshan, and northern part of Longgang districts, and the negative influence was concentrated on Guangming, Pingshan, Yantian and Luohu districts (Fig. 7 a-1). The first three districts are composed of many factories and residences. The increased commercial land may make people avoid traveling long distances for commercial activities and attracting some nearby residents for shopping, which leads to rapid distance decay. However, for the rapid developing urban rural area (Guangming, Yantian and Pingshan districts), an increase in commercial land may promote attracting people at remote villages without commercial facilities. For Luohu, a developed urban business center with many shopping malls, the increase in commercial land would further improve the range of attraction of the places. For outflow, almost of all TAZs showed positive regression coefficients when there was an increase in the percentage of commercial land, and a similar situation was also observed in the industrial, residential and public land (Fig. 7 a-2, b-2, c-2 and d-2). That is, an increase in the four types of land use would motivate people to take activities to a nearby area. For example, an increase in industrial land in the vicinity of a residential-dominated area may induce residents to look for a job near their home. Similarly, an increase in the percentage of industrial and residential land in most TAZs would improve the intensity of distance decay of inflow, and only some TAZs located in Dapeng district appeared a negative effect (Fig. 7 b-1 and c-1). For public land, the positive values of were mainly distributed around the junctional areas among Baoan, Nanshan and Longhua districts, while the negative influences mainly covered the marginal areas of the city (Fig. 7 d-1). A possible explanation is that there are some public attractions in these areas, especially for Yantian and Dapeng districts with some sea beach spots, which generate a global attraction. In contrast to the above four types of land use, the influence of transport land showed a completely different distribution for inflow and outflow. The majority of TAZs

Table 4
Regression results of Inflow_GWR.

Independent variable	Minimum	Lwr quartile	Median	Upr quartile	Maximum	Std
Commercial	−0.087	−0.017	0.004	0.023	0.116	0.027
Industrial	−0.137	0.056	0.069	0.089	0.160	0.030
Residential	−0.488	0.052	0.076	0.099	0.140	0.068
Public	−0.112	−0.019	0.001	0.014	0.086	0.028
Transport	−0.328	−0.104	−0.056	−0.028	0.034	0.055
Land use mix	−0.108	−0.052	−0.027	0.016	0.287	0.052
Road density	−0.125	−0.046	−0.020	0.011	0.073	0.036
Bus stop density	−0.059	−0.018	−0.001	0.014	0.523	0.068
Distance to the nearest subway station (D_1)	−0.662	−0.054	0.005	0.068	0.254	0.126
Distance to the urban center (D_2)	−0.153	−0.101	−0.016	0.171	1.285	0.171
Population	−0.244	−0.082	−0.044	−0.012	0.121	0.057
R^2	0.267					
Adjusted R^2	0.206					

Table 5
Regression results of Outflow_GWR.

Independent variable	Minimum	Lwr quartile	Median	Upr quartile	Maximum	Std
Commercial	−0.015	0.033	0.040	0.048	0.083	0.013
Industrial	−0.027	0.068	0.085	0.106	0.138	0.025
Residential	−0.008	0.075	0.087	0.128	0.219	0.056
Public	−0.172	0.021	0.033	0.043	0.065	0.022
Transport	−0.243	−0.054	−0.040	−0.027	0.002	0.034
Land use mix	−0.093	−0.077	−0.062	−0.034	0.216	0.045
Road density	−0.119	−0.056	0.007	0.024	0.037	0.048
Bus stop density	−0.026	−0.018	0.002	0.026	0.156	0.028
Distance to the nearest subway station (D_1)	−0.242	−0.042	0.047	0.138	0.302	0.124
Distance to the urban center (D_2)	−0.143	−0.078	0.014	0.149	0.273	0.122
Population	−0.175	−0.069	−0.033	−0.015	0.055	0.048
R^2	0.292					
Adjusted R^2	0.231					

produced a negative effect on distance decay (Fig. 7 e-1 and e-2). An increase in transport land is likely to enhance the accessibility of these places and make people travel longer distances. In the southwest corner of Nanshan districts, increased transport land tends to make people move in nearby places. As for land use mix, the significant negative influence was mainly concentrated on Baoan, Nanshan, and Longgang districts, and the positive influence was distributed in Guangming and Dapeng districts (Fig. 7 f-1 and f-2). In urban rural areas, increased mixture of land use may improve the diversity of activities in a local areas, which accelerates distance decay. However, in developed areas, the TAZ with more mixed land use may generate a global attraction and radiation, which results in diminished intensity of distance decay.

With regard to traffic-related variables, the areas with positive influence of road density for inflow mainly surrounded the northwest part of the city (Fig. 7 g-1), which includes many industrial parks or factories, thus an increase in road density may provide a convenient for nearby residents to come for working. The negative values were dominated in the western part of the city, the increased road density may enlarge human activity space, especially in rural areas (Pingshan and Dapeng districts). However, the outflow showed a different spatial distribution. An increase in road density would improve the decay intensity in urban developed center areas while prompting people located in the Baoan, Guangming, Pingshan and Dapeng districts to travel a long distance for taking activities (Fig. 7 g-2). For bus stops, the large positive influences were mainly concentrated in the eastern part of city (Pingshan and Dapeng districts), which covers urban mountains, forests and farms, and the high bus stops density are mainly concentrated in some villages where residents usually have a little activity space, thus having a fast distance decay. The negative values mainly covered the TAZs of two urban center districts (Futian and Luohu) and their adjacent areas (Longhua, Guangming and western part of Longgang). We guess that people living these areas tends to seek a job in developed urban central areas, thus the high-density bus stops may make it convenient to travel a long distance, but the specific reasons need to further investigation. In terms of distance to the nearest subway station, the high positive values were distributed in the urban downtown areas (Nanshan and Futian districts), where subway and other infrastructures are well developed (Fig. 7 i-1 and i-2). Therefore, if an area is far from subway stations, people are likely to take activities in local areas. However, in Guangming, Pingshan and Dapeng districts without subway stations in 2012, the negative influence suggests that the farther an area is from subway stations, the longer the distance is that people need to take.

In addition, the influence of distance between TAZs and the urban center presented a similar spatial distribution characteristic for inflow and outflow. A negative influence appeared around the Futian, Nanshan Luohu and Longhua districts, and the positive values were located in Baoan, Guangming, Pingshan and Dapeng districts (Fig. 7 j-1 and j-2). As aforementioned, the latter four districts have many villages, industrial parks and factories, and people living in these areas have a small activity space, which makes the distance decay fast. However, for urban downtown areas with many commercial, financial, and recreational venues, a global attraction or radiation covers the whole city. For population (Fig. 7 k-1 and k-2), there were similar spatial distribution between inflow and outflow, and more than 75% of TAZs were occupied by negative coefficients. This indicates that the TAZ with larger population tends to be more active, generating a more wide attraction or radiation. However, some positive influences appeared in Yantian and Dapeng districts, these areas are dominated by mountain forests and are sparsely populated, only some villages are inhabited by a small number of residents or farmers with a small activity space.

In summary, the influence of these explanatory variables on the distance decay coefficient showed spatial variation across urban space, and some distinctive differences were observed among urban downtown, suburban, and rural areas. This knowledge provides an insight into the urban distance decay of human movements at a more microscopic scale, which has a referential value for urban traffic management and planning. For example, it may be helpful for improving the forecasting of trip generation by incorporating these varying decay coefficients into the famous land use and transport model.

5. Conclusion

Recent technological development makes it effortless to collect large-scale human space–time trajectory datasets, which present new opportunities to understand or rethink traditional research questions on human mobility at a comprehensive spatiotemporal scale. A classic issue is human spatial interaction that describes the human flow among different places. This work attempts to fill up a gap in the analysis of the spatial heterogeneity of distance decay of spatial interaction in an urban space by using a large human sensing dataset. The main contributions of this study are as follows.

First, we extracted the urban spatial interaction matrix from massive mobile phone data from Shenzhen, China. We utilized a power-law function to fit the distance decay coefficients of inflow and outflow for a place. The large values of decay coefficients were mainly concentrated on the northern part of the city, whereas low values dominated in the urban southern areas. The global Moran's I test indicated that the spatial distribution of the decay coefficients of inflow and outflow showed remarkable spatial cluster patterns.

Second, the traditional OLS and GWR models were used to quantify the relationship between decay coefficients and several explanatory variables related to land use and traffic. GWR showed a remarkable improvement in fitting effectiveness compared with the OLS model. Furthermore, the varying regression coefficients revealed the spatial varying of the influence of land use and traffic on the distance decay of spatial interaction.

However, this study has several limitations that should be

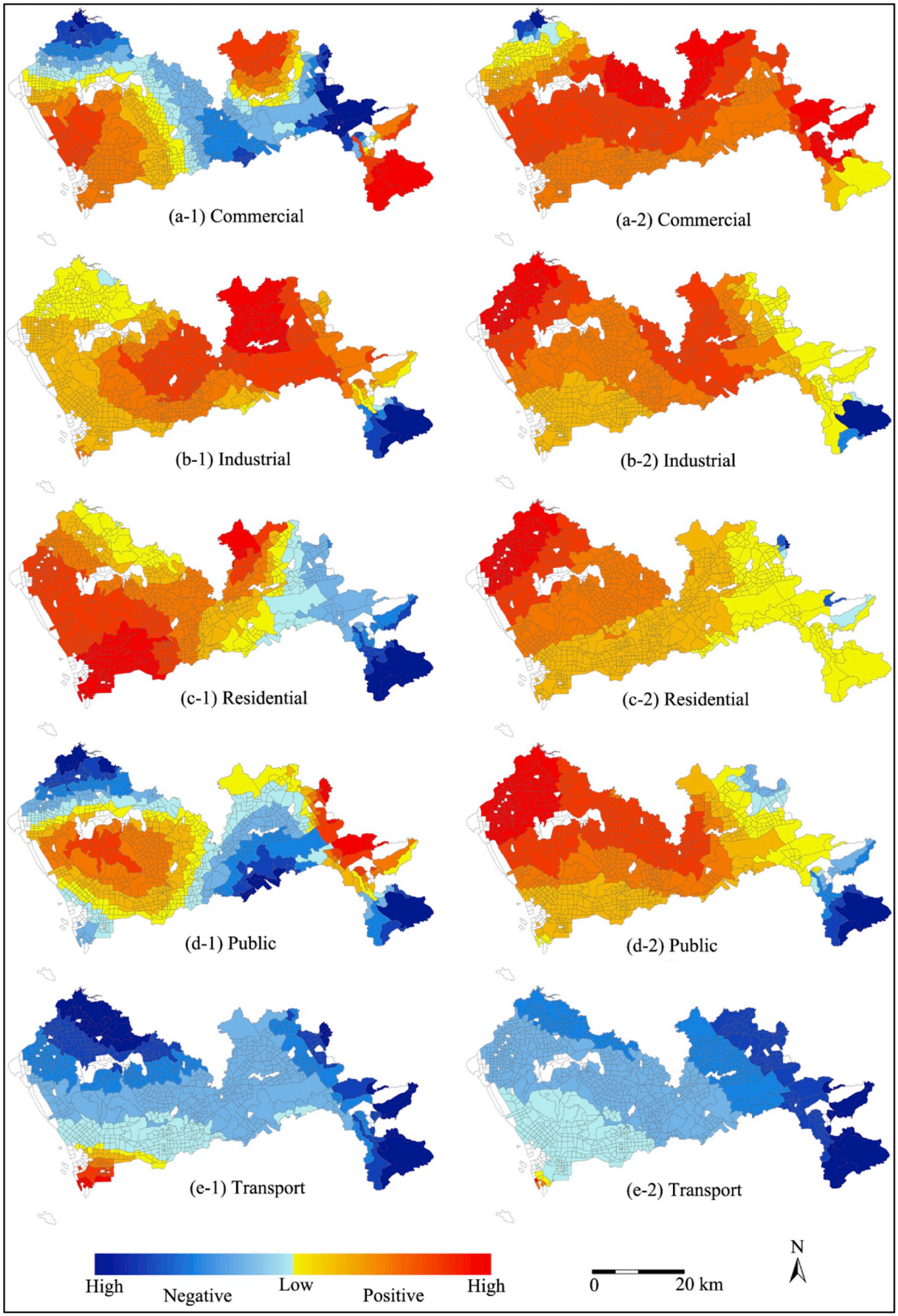

Fig. 7. Spatial distribution of varying regression coefficients. The left column represents inflow, and the right column represents outflow.

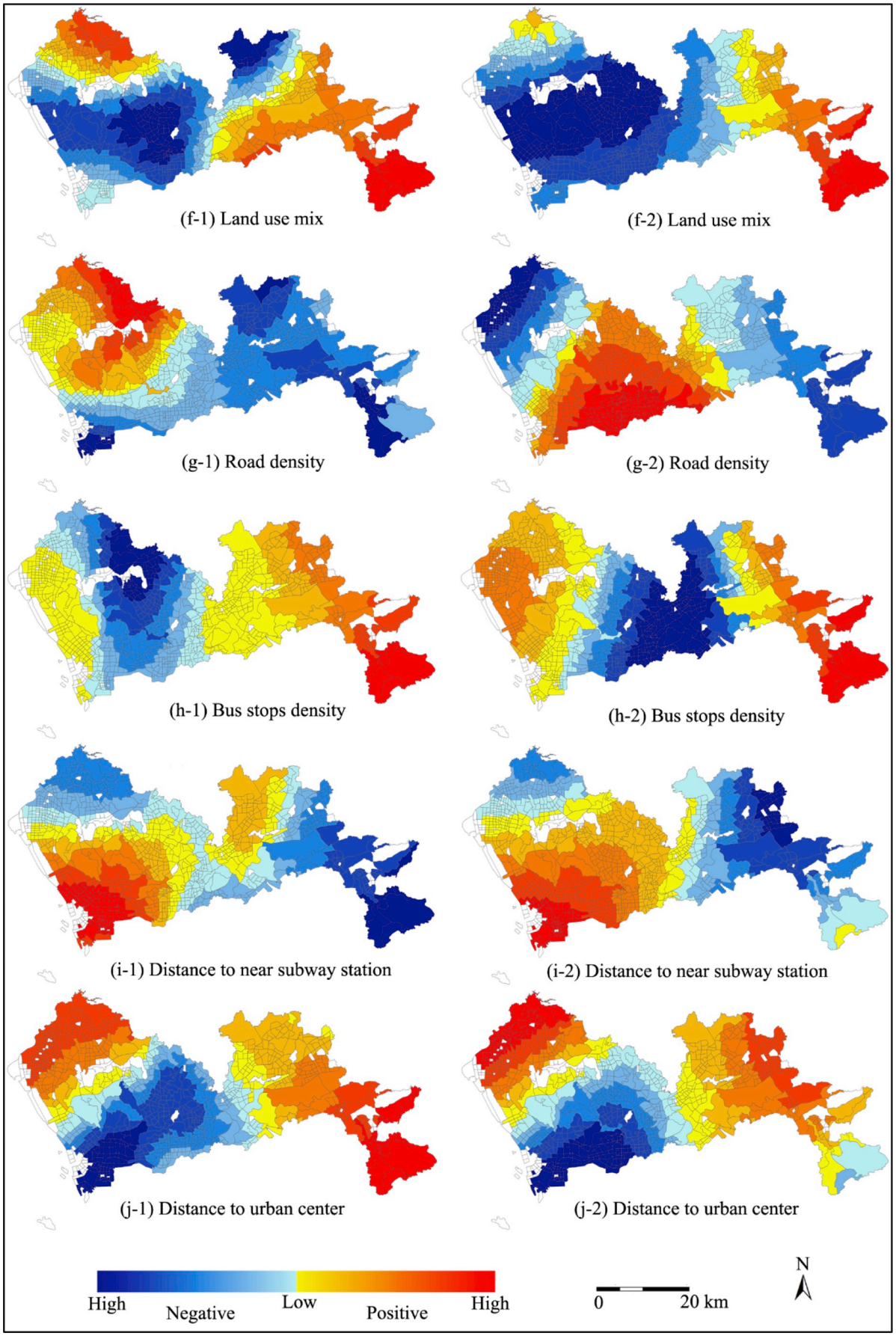

Fig. 7. (*continued*)

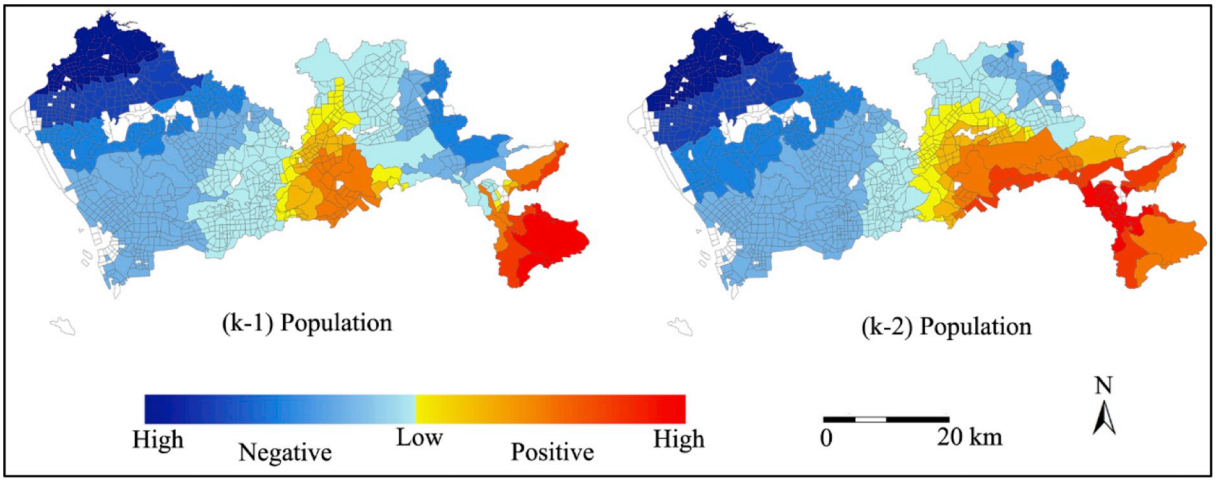

Fig. 7. (*continued*)

considered in future work. First, it considered the spatial variation when fitting decay coefficients but ignored the time factor of spatial interaction. It would be interesting to combine temporal variation for improved understanding of the spatiotemporal characteristics of distance decay of spatial interaction. Second, although the regression results show that there are spatial variations existing in distance decay coefficients, the low adjusted R^2 indicates the selected land use and traffic-related explanatory variables can only explain the about 20% of variability of the decay coefficients, which demonstrates that these explanatory variables are not the dominant influence factors on distance decay. In fact, the distance decay of a place could be affected by other factors such as socioeconomic characteristics and urban spatial structure (Fotheringham, 1981; Hipp and Boessen, 2017), which are also important dimensions affecting human spatial interaction. For example, a place with well job-housing balance may have less spatial interaction with other places, and residents may have little activity space, resulting in faster distance decay. Therefore, it still needs to further investigate the influence of other factors on distance decay. In addition, experiments should be conducted in other cities to check if consistent results could be achieved.

Acknowledgements

This research was jointly supported by the National Natural Science Foundation of China (Nos. 41801373, 41771473, 41771441, 41801372, 51708426), China Postdoctoral Science Foundation (Nos. 2017M623112, 2018M632860), Fundamental Research Funds for the Central Universities (Grants GK201803049, 2042017kf0235), and National Key R & D Plan (2017YFC1405302, 2017YFB0503802), Special Funds for Basic Scientific Research Business in Central Colleges and Universities, (Independent Scientific Research Project of Wuhan University in 2018, NO. 2042018kf0250), Shaanxi science and technology program (NO. 2019ZDLSF07-04), and the Open Fund of Key Laboratory of Urban Land Resources Monitoring and Simulation, Ministry of Land and Resources (KF-2018-03-006).

Conflicts of interest

The authors declare no conflict of interest.

References

Burnham, K.P., Anderson, D.R., 2004. Multimodel inference: understanding AIC and BIC in model selection. Sociol. Methods Res. 33 (2), 261–304.
Chen, Y., 2015. The distance-decay function of geographical gravity model: power law or exponential law? Chaos, Solitons Fractals 77, 174–189.
de Vries, J.J., Nijkamp, P., Rietveld, P., 2009. Exponential or power distance-decay for commuting? An alternative specification. Environ. Plan. A 41 (2), 461–480.
Fang, Z., Yang, X., Xu, Y., Shaw, S.-L., Yin, L., 2017. Spatiotemporal model for assessing the stability of urban human convergence and divergence patterns. Int. J. Geogr. Inf. Sci. 31 (11), 2119–2141.
Fotheringham, A.S., 1981. Spatial structure and distance decay parameters. Ann. Assoc. Am. Geogr. 71 (3), 425–436.
Fotheringham, A.S., O'Kelly, M.E., 1989. Spatial Interaction Models: Formulations and Applications. vol. 1 Kluwer Academic Publishers, Dordrecht.
Gao, S., Liu, Y., Wang, Y., Ma, X., 2013. Discovering spatial interaction communities from mobile phone data. Trans. GIS 17 (3), 463–481.
González, M.C., Hidalgo, C.A., Barabási, A.-L., 2008. Understanding individual human mobility patterns. nature 453, 779.
Hägerstraand, T., 1970. What about people in regional science? Pap. Reg. Sci. 24 (1), 7–24.
Halás, M., Klapka, P., Kladivo, P., 2014. Distance-decay functions for daily travel-to-work flows. J. Transp. Geogr. 35, 107–119.
Han, S.Y., Tsou, M.-H., Clarke, K.C., 2018. Revisiting the death of geography in the era of Big Data: the friction of distance in cyberspace and real space. Int. J. Digital Earth 11 (5), 451–469.
Hipp, J.R., Boessen, A., 2017. The shape of mobility: measuring the distance decay function of household mobility. Prof. Geogr. 69 (1), 32–44.
Huff, D.L., 1963. A probabilistic analysis of shopping center trade areas. Land Econ. 39 (1), 81–90.
Kang, C., Ma, X., Tong, D., Liu, Y., 2012. Intra-urban human mobility patterns: an urban morphology perspective. Phys. A 391 (4), 1702–1717.
Kang, C., Sobolevsky, S., Liu, Y., Ratti, C., 2013. Exploring human movements in Singapore: A comparative analysis based on mobile phone and taxicab usages. In: Proceedings of the 2nd ACM SIGKDD International Workshop on Urban Computing. ACM, Chicago, Illinois, pp. 1–8.
Kong, X., Liu, Y., Wang, Y., Tong, D., Zhang, J., 2017. Investigating public facility characteristics from a spatial interaction perspective: a case study of Beijing hospitals using taxi data. ISPRS Int. J. Geo-Inf. 6 (2).
Kordi, M., Fotheringham, A.S., 2016. Spatially weighted interaction models (SWIM). Ann. Am. Assoc. Geogr. 106 (5), 990–1012.
Lee, K.H., Schuett, M.A., 2014. Exploring spatial variations in the relationships between residents' recreation demand and associated factors: a case study in Texas. Appl. Geogr. 53, 213–222.
Li, Y., Liu, L., 2012. Assessing the impact of retail location on store performance: a comparison of Wal-Mart and Kmart stores in Cincinnati. Appl. Geogr. 32 (2), 591–600.
Liang, X., Liu, Y., Qiu, T., Jing, Y., Fang, F., 2018. The effects of locational factors on the housing prices of residential communities: the case of Ningbo, China. Habitat Int. 81, 1–11.
Liu, Y., Kang, C., Gao, S., Xiao, Y., Tian, Y., 2012. Understanding intra-urban trip patterns from taxi trajectory data. J. Geogr. Syst. 14 (4), 463–483.
Liu, Y., Sui, Z., Kang, C., Gao, Y., 2014. Uncovering Patterns of Inter-Urban Trip and Spatial Interaction from Social Media Check-In Data. PLoS ONE 9 (1), e86026. https://doi.org/10.1371/journal.pone.0086026.
Liu, X., Gong, L., Gong, Y., Liu, Y., 2015a. Revealing travel patterns and city structure with taxi trip data. J. Transp. Geogr. 43, 78–90.
Liu, Y., Liu, X., Gao, S., Gong, L., Kang, C., Zhi, Y., Chi, G., Shi, L., 2015b. Social sensing: a new approach to understanding our socioeconomic environments. Ann. Assoc. Am. Geogr. 105 (3), 512–530.
Louail, T., Lenormand, M., Picornell, M., Cantú, O.G., Herranz, R., Frias-Martinez, E., Ramasco, J.J., Barthelemy, M., 2015. Uncovering the spatial structure of mobility networks. Nat. Commun. 6, 6007.
Ma, X., Liu, C., Wen, H., Wang, Y., Wu, Y.-J., 2017. Understanding commuting patterns using transit smart card data. J. Transp. Geogr. 58, 135–145.
Martínez, L.M., Viegas, J.M., 2013. A new approach to modelling distance-decay functions for accessibility assessment in transport studies. J. Transp. Geogr. 26, 87–96.

Nakaya, T., Fotheringham, S., Charlton, M., Brunsdon, C., 2009. Semiparametric Geographically Weighted Generalised Linear Modelling in GWR 4.0.
Qian, X., Ukkusuri, S.V., 2015. Spatial variation of the urban taxi ridership using GPS data. Appl. Geogr. 59, 31–42.
Roy, J.R., Thill, J.-C., 2004. Spatial interaction modelling. Pap. Reg. Sci. 83 (1), 339–361.
Sen, A., Smith, T.E., 2012. Gravity Models of Spatial Interaction Behavior. Springer Science & Business Media.
Shaw, S.-L., Tsou, M.-H., Ye, X., 2016. Editorial: human dynamics in the mobile and big data era. Int. J. Geogr. Inf. Sci. 30 (9), 1687–1693.
Siła-Nowicka, K., Fotheringham, A.S., 2018. Calibrating Spatial Interaction Models from GPS Tracking Data: An Example of Retail Behaviour. Computers, Environment and Urban Systems.
Song, C., Qu, Z., Blumm, N., Barabási, A.-L., 2010. Limits of predictability in human mobility. Science 327 (5968), 1018–1021.
Stewart, Fotheringham A., Charlton, M., Brunsdon, C., 1996. The geography of parameter space: an investigation of spatial non-stationarity. Int. J. Geogr. Inf. Syst. 10 (5), 605–627.
Suárez-Vega, R., Gutiérrez-Acuña, J.L., Rodríguez-Díaz, M., 2015. Locating a supermarket using a locally calibrated Huff model. Int. J. Geogr. Inf. Sci. 29 (2), 217–233.
Sui, D., Shaw, S.-L., 2018. Human dynamics in smart and connected communities. Comput. Environ. Urban. Syst. 72, 1–3.
Tobler, W.R., 1970. A computer movie simulating urban growth in the detroit region. Econ. Geogr. 46 (sup1), 234–240.
Tu, W., Cao, R., Yue, Y., Zhou, B., Li, Q., Li, Q., 2018. Spatial variations in urban public ridership derived from GPS trajectories and smart card data. J. Transp. Geogr. 69, 45–57.
Ullman, E.L., 1980. Geography as Spatial Interaction. University of Washington Press.
Wang, Y., Jiang, W., Liu, S., Ye, X., Wang, T., 2016. Evaluating trade areas using social media data with a calibrated Huff model. ISPRS Int. J. Geo Inf. 5 (7).
Xu, Y., Shaw, S.-L., Zhao, Z., Yin, L., Fang, Z., Li, Q., 2015. Understanding aggregate human mobility patterns using passive mobile phone location data: a home-based approach. Transportation 42 (4), 625–646.
Xu, Y., Shaw, S.-L., Zhao, Z., Yin, L., Lu, F., Chen, J., Fang, Z., Li, Q., 2016. Another tale of two cities: understanding human activity space using actively tracked cellphone location data. Ann. Am. Assoc. Geogr. 106 (2), 489–502.
Yang, X., Fang, Z., Yin, L., Li, J., Zhou, Y., Lu, S., 2018a. Understanding the spatial structure of urban commuting using mobile phone location data: a case study of Shenzhen, China. Sustainability 10 (5), 1435.
Yang, Z., Franz, M.L., Zhu, S., Mahmoudi, J., Nasri, A., Zhang, L., 2018b. Analysis of Washington, DC taxi demand using GPS and land-use data. J. Transp. Geogr. 66, 35–44.
Yin, L., Wang, Q., Shaw, S.-L., Fang, Z., Hu, J., Tao, Y., Wang, W., 2015. Re-identification risk versus data utility for aggregated mobility research using mobile phone location data. PLoS One 10 (10), e0140589.
Yuan, Y., Raubal, M., 2012. Extracting dynamic urban mobility patterns from mobile phone data. In: International Conference on Geographic Information Science. Springer, pp. 354–367.
Yue, Y., Wang, H.-d., Hu, B., Li, Q.-q., Li, Y.-g., Yeh, A.G.O., 2012. Exploratory calibration of a spatial interaction model using taxi GPS trajectories. Comput. Environ. Urban. Syst. 36 (2), 140–153.